Laser-induced-damage threshold of periodically poled lithium niobate for 1030 nm femtosecond laser pulses at 100 kHz and 75 MHz

I. Pipinytė, R. Grigonis, K. Stankevičiūtė, S. Kičas, R. Drazdys, et al.

I. Pipinytė, R. Grigonis, K. Stankevičiūtė, S. Kičas, R. Drazdys, R. C. Eckardt, V. Sirutkaitis, "Laser-induced-damage threshold of periodically poled lithium niobate for 1030 nm femtosecond laser pulses at 100 kHz and 75 MHz," Proc. SPIE 8786, Pacific Rim Laser Damage 2013: Optical Materials for High Power Lasers, 87861N (9 July 2013); doi: 10.1117/12.2020379

Event: SPIE/SIOM Pacific Rim Laser Damage: Optical Materials for High-Power Lasers, 2013, Shanghai, China

Laser-induced-damage threshold of periodically poled lithium niobate for 1030 nm femtosecond laser pulses at 100 kHz and 75 MHz

I. Pipinytė[1], R. Grigonis[1], K. Stankevičiūtė[1], S. Kičas[2], R. Drazdys[2], R. C. Eckardt[3], V. Sirutkaitis[1]

[1] Vilnius University Laser Research Center, Saulėtekio av. 10, 10223 Vilnius, Lithuania
[2]Center for physical sciences and technology, Savanorių pr. 231, 02300 Vilnius, Lithuania
[3]Gooch and Housego (Ohio), 676 Alpha Drive, Highland Hts, Ohio, 44143 U.S.A.

ABSTRACT

We report laser-induced damage threshold (LIDT) measurements of periodically poled lithium niobate (PPLN) and magnesium-oxide-doped PPLN (MgO:PPLN) in the femtosecond pulse duration regime at 1030 nm with 100 kHz and 75 MHz repetition rate. PPLN and MgO:PPLN crystals with broadband Nb_2O_5/SiO_2 AR coatings for 1.4 – 1.8 um spectral range were used. S-on-1 test for LIDT measurements were performed. S was equal to 10^6 and $4.56*10^{10}$ pulses for 100 kHz CPA laser system and 75 MHz oscillator, respectively. Evaluated LIDT was 20 mJ/cm^2 for 290 fs pulses at 100 kHz repetition rate and 0.63 mJ/cm^2 for 105 fs pulses at 76 MHz repetition rate.

Keywords: periodically poled lithium niobate, laser-induced-damage-threshold, Yb:KGW laser

1. INTRODUCTION

Recently, tunable in broad spectral range femtosecond nonlinear optical devices, like optical parametric generators and oscillators (OPG and OPO respectively), are important elements in various applications such as medicine, telecommunications, biology, chemistry. Most radiation properties of these coherent light sources depend on the choice of pumping source and nonlinear material. The use of periodically poled lithium niobate (PPLN) as nonlinear material for the mid-infrared OPG and OPO systems become very desirable, because its advantageous properties. Most important characteristics are a relatively large effective nonlinear coefficient ($d_{eff} \approx 17$ pm/V) and a wide transmission range (0.42 – 5.2 μm). The large nonlinear coefficient allows effective conversion with relatively short structures, which is important for group-velocity-mismatch concerns of short-duration pulses. However, lithium niobate crystals have a low laser-induced damage threshold (LIDT). If threshold energy density (E_{th}) is exceeded, crystal can be permanently damaged and become unsuitable for further use. Consequently, LIDT is a significant parameter that limits the potential use of the pumping intensity for OPG and OPO, and the maximum output power of these optical devices. Thus, knowledge of material optical resistance limits is particularly important before applying it to the new optical system. There are some reports on PPLN LIDT measurements for femtosecond pulses generated by Ti:sapphire lasers at 800 nm [1, 2]. Under a single shot LIDT was 2.82 J/cm^2 for 90 fs long pulses [1] and 2 J/cm^2 for 50 fs [2]. E_{th} was found to decrease with increase in the pulse number (N): $E_{th}= 0.52 \pm 0.06$ J/cm^2 for N>80 [1] and 0.8 J/cm^2 for N=1000 [2] due to accumulation and incubation effects [1, 3]. Currently commonly used optical parametric devices with lithium niobate structures are pumped by fundamental Ti: sapphire laser output [4-11]. However due to recent development of ytterbium lasers and the possibility to create more effective optical parametric devices pumped by their radiation rather than Ti:sapphire lasers, it became important to know LIDT for those lasers pulses at 1030 nm.

In our investigations, we developed two different optical systems: single-pass optical parametric generator (SOPG) (Fig. 1. a)) and synchronously pumped optical parametric oscillator (SPOPO) (Fig. 1. b)) [12]. As a pump source for SOPG we used Yb:KGW laser system generating IR (1030 nm) pulses of ~ 300 fs pulse duration and maximum pulse energy up to 30 μJ at 100 kHz repetition rate. The pump beam was focused in a nonlinear medium to 138 μm diameter spot by 30 cm focus length lens. As a nonlinear material we used 0.5 mm thick and 8 mm long PPLN crystal with different grating periods ranging from 25 μm to 31.5 μm in 0.25 μm step, resulting in a possibility to get a signal in ~ 1.35 – 2.0 μm spectral range. For SPOPO pumping we used Yb:KGW oscillator, which produced IR pulses of ~100 fs pulse duration and maximum pulse energy up to ~ 50 nJ at 75 MHz repetition rate. In this case, pump beam was focused to 52.6 μm diameter spot. As nonlinear materials we used 1.5 mm long PPLN and MgO:PPLN structures with

Pacific Rim Laser Damage 2013: Optical Materials for High Power Lasers,
edited by Jianda Shao, Takahisa Jitsuno, Wolfgang Rudolph, Proc. of SPIE Vol. 8786,
87861N · © 2013 SPIE · CCC code: 0277-786X/13/$18 · doi: 10.1117/12.2020379

different grating periods ranging from 25 μm to 31.5 μm in 0.25 μm step and from 28.5 μm to 31.5 μm in 0.5 μm step, respectively. In order to avoid a photorefractive effect, PPLN crystals were heated to 120 °C, while MgO:PPLN just to 30 °C as it was more resistant for this phenomenon.

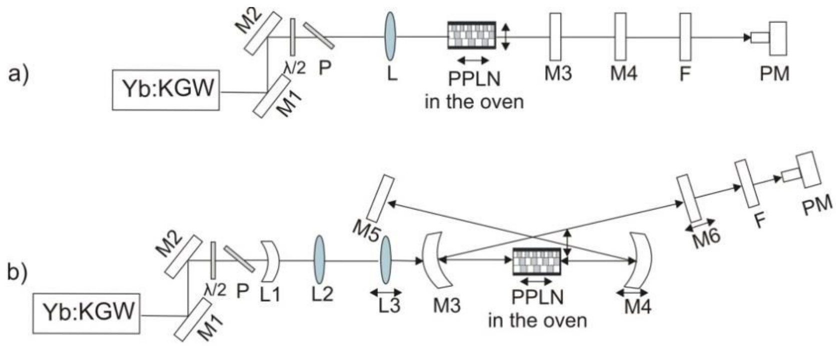

Fig. 1. Experimental setup of: 1) travelling wave optical parametric generator and 2) synchronously pumped optical parametric oscillator. Here: M1-M6 – mirrors, λ/2 – half wavelength phase plate, P – polarizer, L1-L2 – telescope, L, L3 – lens, F- filter, PM – power meter

2. AR COATINGS OF CRYSTALS

As mentioned above, lithium niobate is highly transparent in a wide spectral range (0.42 – 5.2 μm). However, it is very important in femtosecond optical systems to minimize the losses of interacting waves. Thus, in our case it was necessary to deposit antireflection (AR) coatings on the crystal surfaces in order to reduce reflectance losses of pump and signal waves. For this, broadband Nb_2O_5/SiO_2 AR coatings on our crystals for ~ 1.4 – 1.8 μm spectral range and 1030 nm pump wavelength were made. Crystals were deposited by using a modified Ion beam sputtering (IBS) technique presented on Fig. 2. This method is known to fulfill demanding requirements and ensuring high quality of broadband coatings used in femtosecond optical systems [13].

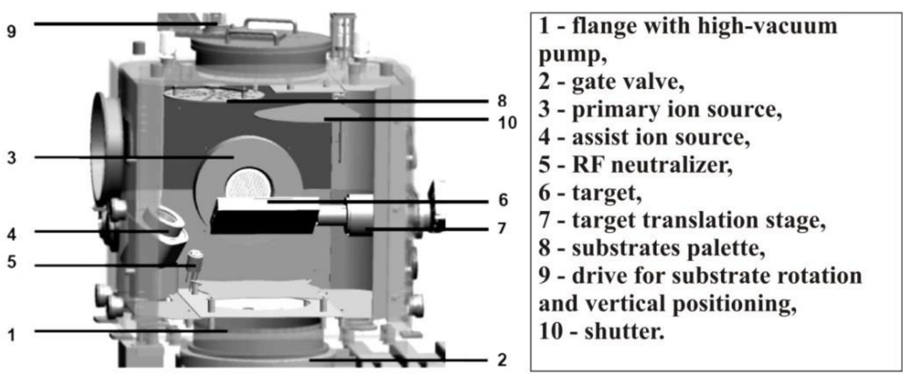

Fig. 2. Interior view of process chamber

The apparatus was equipped with a combination of cryo and vacuum pumps and resulted in a vacuum base pressure of 4×10^{-5} Pa. Before the deposition process, the vacuum chamber was heated to 50 °C for 1 hour. To remove the impurity layer, presputtering of targets by argon ion beam source was used before the deposition of each layer. A radio-frequency grid-system-based ion beam source was used to strike a plane zone target consisting of two different materials: high refractive index (Nb) and low refractive-index (Si) (Fig. 3.) at an angle of incidence of 57 degrees. Dispersion curves of refractive indices of selected materials were experimentally estimated before deposition process. Insignificant absorption of materials in the visible spectral region was detected and therefore it can be neglected.

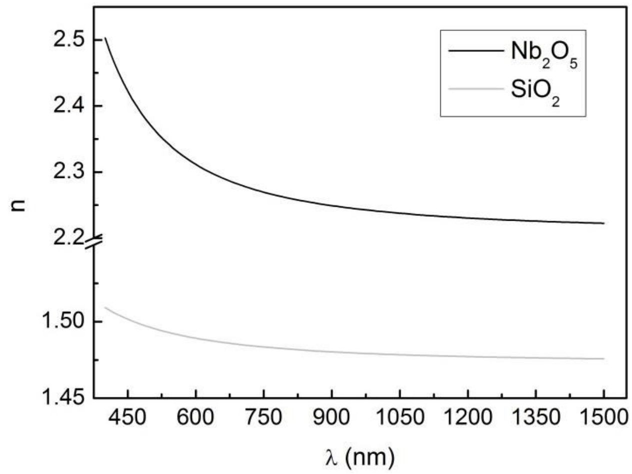

Fig. 3. Nb_2O_5 and SiO_2 dispersion

A radio-frequency driven neutralizer produced additional electrons to antagonize charging effects caused by positively charged gas ions in the chamber. During the process, 100 sccm of oxygen gas was supplied towards the substrate to ensure complete oxidation of the growing coating. This results in working pressure increase up to 3×10^{-3} Pa. Ion accelerating voltage of the main argon ion source were set to 1200 V and deposition speeds of 1 Å/s for low and 0.6 Å/s for high-refractive-index materials were achieved respectively. Alternating layers of Nb_2O_5 and SiO_2 were deposited by shifting ion–metal interaction zone across Nb/Si target mounted on a linear translation stage. The films were deposited on substrates held in a circular rack, which was rotated around its axis at a speed of 20 rpm to improve thickness distribution uniformity. The thicknesses of growing layers were monitored by an integrated broadband transmission optical monitoring system.

Theoretical and measured reflection spectrums of coatings are shown in Fig. 4. Experimentally obtained curve was measured with optical parametric amplifier OPerA Solo in 1180 – 1600 nm spectral range. Results of coatings test show that small losses for signal and pump waves (R<0.5 %) were achieved.

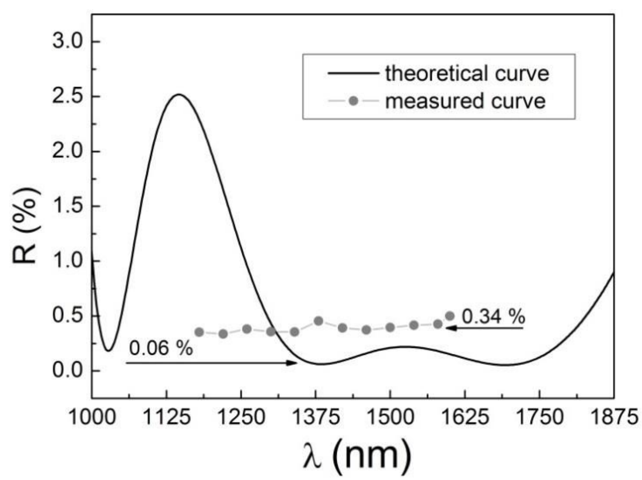

Fig. 4. Theoretical and experimental reflectance spectrums of crystal's AR coatings

3. LIDT MEASUREMENT

We performed S-on-1 (more precisely it is R-on-1 test as laser pulse energy was ramped from the smallest values up to LIDT irradiating the same site of the crystal) LIDT measurements in our described optical systems while crystals were exposed by finite number of laser pulses. S was equal to 10^6 and $4.56*10^{10}$ pulses for 100 kHz CPA Yb:KGW laser system and 75 MHz Yb:KGW oscillator, respectively. All other parameters: crystal temperature, pump beam focusing remained the same as they were planned for use in experiments. The experimental setup for the laser-induced surface damage threshold measurements is presented in Fig. 5. The energy of the pump pulse was changed continuously with the combination of a half-wave plate and a polarizer. LIDT was indicated by drop in transmission. For LIDT tests 8 mm and 1.5 mm long PPLN and 1.5 mm long MgO:PPLN crystals with broadband Nb_2O_5/SiO_2 AR coatings and one 1.5 mm long uncoated MgO:PPLN sample were used.

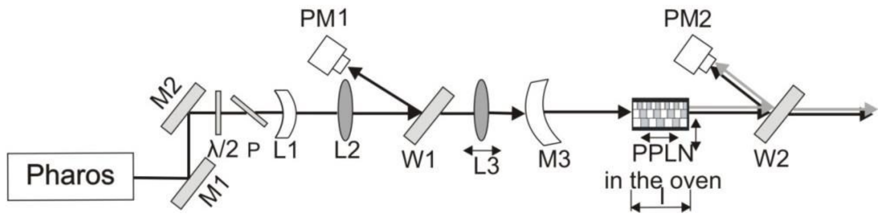

Fig. 5. Experimental setup of LIDT measurements: M1–M4 mirrors, L1-L2 – telescope, λ/2 – half wavelength phase plate, P – polarizer, L3 – lens, PM – power meter, l – crystal length, W – wedge. Here: black arrow – pump (1030 nm), grey arrow – second harmonic of the pump (515 nm)

At first, we did LIDT measurements of 8 mm long PPLN crystal pumped by CPA Yb:KGW laser output. For this test, we pointed pumping radiation into the crystal edge to ensure not to damage areas, where were grating periods needed in our later study. We also used selective filters in order to avoid fundamental and second harmonic output behind the crystal and measure just the energy of signal beam. The damage on crystal surface was made at pumping energy's value 3.03 μJ. Hence, damage threshold of the PPLN crystal using 10^6 pulses with 290 fs duration at repetition rate 100 kHz was ~ 0.02 J/cm^2 (Fig. 6.).

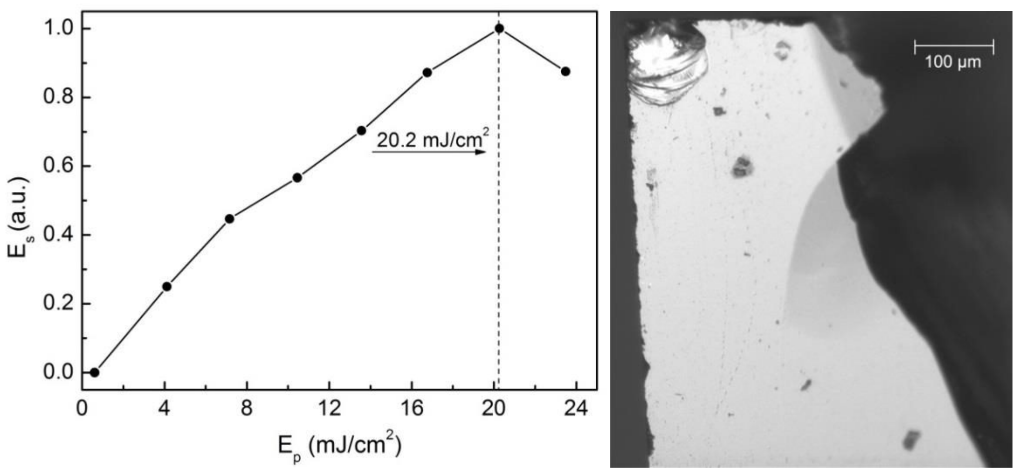

Fig. 6. Comparative signal wave's energy (E_s) as a function of pump fluence (E_p) (left), and a view of the laser initiated surface damage on PPLN (obtained with optical microscope) (right)

Subsequently, LIDT measurements in the optical system with high repetition rate Yb:KGW oscillator were performed. For estimation of the threshold value we used four surface points of PPLN, two of MgO:PPLN crystals with AR coatings and two points of MgO:PPLN crystal without AR coatings. Results showed, that minimal energy fluency, which corresponded to the optical damage threshold of PPLN sample, was 0.63 mJ/cm^2 (Fig. 7 a)). This was led to the fact that the pumping power in our developing SPOPO system was limited to ~1W, while pumping source could generate 4W average power. Thus, LIDT of nonlinear material is an important factor, which limits the maximum output and efficiency of the SPOPO system. The LIDT of MgO:PPLN was slightly higher and equal to 0.79 mJ/cm^2 (Fig. 7 b)). The crystal without AR coating was most resistance to optical damage as value of its LIDT was 0.84 mJ/cm^2.

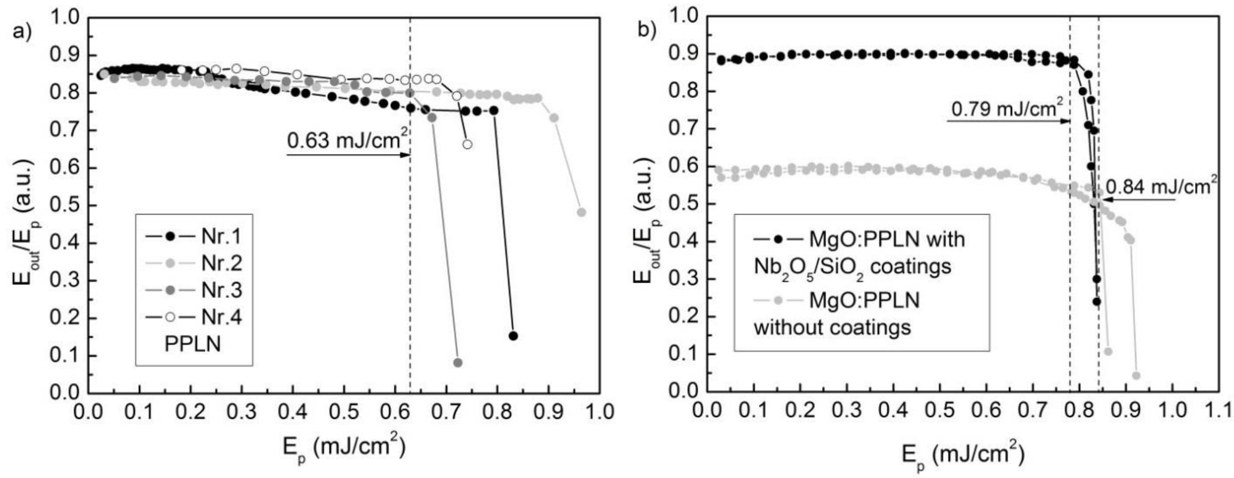

Fig. 7. Ratio of output energy and pump energy from pump energy flow using: a) PPLN crystal with NbO_2O_5/SiO_2 coatings and b) MgO:PPLN crystals with and without coatings

Main data of LIDT measurements are summarized in Table 1. Table shows the LIDT value, obtained using high repetition rate (76 MHz) Yb:KGW laser radiation, was about 30 times lower than that, which was achieved by 100 kHz repetition rate CPA Yb:KGW laser output. It can be seen that the threshold fluence was influenced by the number of pulses irradiated the crystal surface. Thus, it can be explained by an incubation effect, which may occur for several reasons. At first, the material could experience structural changes, i.e. formation of laser induced defects, which could increase absorption of photons. Accumulation of heat could be another cause of the incubation: energy of each pulse could be partially absorbed by defects in material, i.e. could be converted into heat. If the pulse repetition rate is high, the material cannot cool until the next pulse reaches that crystal surface area. Consequently, the heat accumulates and reduces material resistance to laser radiation.

Table 1. Parameters and results of LIDT measurements

	PPLN	**PPLN**	**MgO:PPLN**	**MgO:PPLN without coatings**
Crystal length	8 mm	1.5 mm	1.5 mm	1.5 mm
Pulse duration	290 fs	105 fs	105 fs	105 fs
Pulse repetition rate	100 kHz	76 MHz	76 MHz	76 MHz
Beam spot diameter	138 μm	52.6 μm	52.6 μm	52.6 μm
Maximum impulse energy	30 μJ	52.6 nJ	52.6 nJ	52.6 nJ
Pulse number	$2*10^6$	$4.56*10^{10}$	$4.56*10^{10}$	$4.56*10^{10}$
LIDT	20 mJ/cm^2 (190.5 GW/cm^2)	0.63 mJ/cm^2 (6 GW/cm^2)	0.79 mJ/cm^2 (7.5 GW/cm^2)	0.84 mJ/cm^2 (8 GW/cm^2)

Fig. 8 illustrates images of LIDT on crystal surface, obtained by different fluence levels. In case of PPLN crystal (Fig. 8 a-d), the smallest and most symmetric damage zone size was obtained by lowest value of fluence (Fig. 8 d)). Here diameter of damage spot is equal to diameter of focal spot (at $1/e^2$ maximum intensity). Dimensions of damage area become bigger than focus beam size and not symmetrical, than surfaces damage are obtained by higher energy levels. As fluence increases, outer fronts of the beam become stronger, so it is possible to get larger damage areas. These zones also can spread and become irregular shapes due to the energy released in local absorption centers, which are close to the irradiated surface.

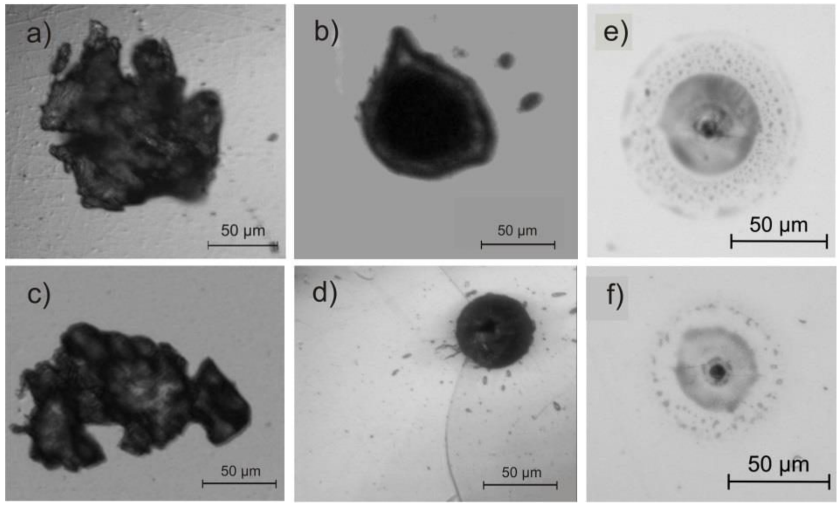

Fig. 8. a) – d) images of optical damage on PPLN surface. Damages were obtained by a) 0.88 mJ/cm^2, b) 0.79 mJ/cm^2, c) 0.68 mJ/cm^2, d) 0.63 mJ/cm^2. e) – f) images of optical damage on MgO:PPLN without AR coatings surface: e) 0.84 mJ/cm^2, f) 0.9 mJ/cm^2

CONCLUSIONS

We measured lithium niobate surface damage thresholds observed in two different optical systems. Measurements showed that damage threshold for S-on-1 test with Yb:KGW laser 290 fs pulse duration S=10^6 pulses at 100 kHz repetition rate was 0.02 J/cm^2 for PPLN. LIDT, obtained by 105 fs pulse duration S=4.56 *10^{10} pulses at 76 MHz repetition rate, was equal to 0.63 mJ/cm^2 for PPLN and 0.79 mJ/cm^2 for MgO:PPLN. Consequently, we demonstrated that pulse repetition rate of the femtosecond pulses has a significant impact on the surface damage threshold value for periodically poled lithium niobate structures.

ACKNOWLEDGEMENTS

This work was partly supported by the Lithuanian Agency for Science, Innovation and Technology (Grant No. 31V-35, project MEGAOPO).

REFERENCES

[1] Chen, H. Chen, X., Zhang, Y. and Xia, Y., "Ablation Induced by Single- and Multiple-Femtosecond Laser Pulses in Lithium Niobate", Las. Phys. 17(12), 1378-1381 (2007).

[2] Yu, B. Lu, P., Dai, N., Li, Y., Wang, X., Wang, Y. and Zheng, Q., "Femtosecond laser-induced sub-wavelength modification in lithium niobate single crystal", J. Opt. A: Pure Appl. Opt.10, 1-5 (2008).

[3] Ashkenasi, D., Lorenz, M., Stoian, R. and Rosenfeld, A., "Surface damage threshold and structuring of dielectrics using femtosecond laser pulses: the role of incubation", Appl. Surf. Sci. 150, 101-106 (1999).

[4] Burr, K. C., Tang, C. L., Arbore, M. A., and Fejer, M. M., "Broadly tunable mid-infrared femtosecond optical parametric oscillator using all-solid-state-pumped periodically poled lithium niobate", Opt. Lett. 22(19), 1458-1460 (1997).

[5] McGowan, C. Reid, D.T., Penman, Z. E., Ebrahimzadeh, M., Sibbett, W. and Jundt, D. H., "Femtosecond optical parametric oscillator based on periodically poled lithium niobate", J. Opt. Spc. Am. 15, 694-701 (1998).

[6] Zhang, X. P., Hebling, J., Bartels, A., Nau, D., Kuhl, J., Ruhle, W. W. and Giessen, "1-GHz-repetition-rate femtosecond optical parametric oscillator", Appl. Phys. Lett. 80(11), 1873-1875 (2002).

[7] Andres, T., Haag, P., Zelt, S., Meyn, J. -P., Borsutzky, A., Beigang, R. and Wallenstein, R., "Synchronously pumped femtosecond optical parametric oscillator of congruent and stoichiometric MgO-doped periodically poled lithium niobate", Appl. Phys. B 76, 241–244 (2003).

[8] Meng, X., Diels, J. -D., Kuehlke, D., Batchko, R. and Byer, R.,"Bidirectional, synchronously pumped, ring optical parametric oscillator", Opt. Lett. 26(5), 265-267 (2001).

[9] Jiang -Feng, Z., Xin, Z., Hao, T., Jing-Hua, S. and Zhi-Yi, W., "Synchronously pumped optical parametric oscillator based on MgO doped periodically poled $LiNbO_3$", Chin.Phys. Lett. 24(9), 2603-2605 (2007).

[10] Xin Z., Jiang-Feng, Z., BinBin, Z. and ZhiYi, W., "Synchronously pumped femtosecond optical parametric oscillator at 1053 nm", Sci.Chin.Press. 52(8), 1187-1190 (2009).

[11] Sun, J., Gale, B. J. S. and Reid, D.T., "Dual-color operation of a femtosecond optical parametric oscillator exhibiting stable relative carrier-envelope phase-slip frequencies", Opt. Lett. 31(13), 2021-2023 (2006).

[12] Stankevičiūtė, K., Pipinytė, I., Stasevičius, I., Vengelis, J., Valiulis, G., Grigonis, R., Vengris, M., Bardauskas, M., Giniūnas, L., Balachninaite, O., Eckard, R. C. and Sirutkaitis, V., "Femtosecond optical parametric oscillators sunchronously pumped by Yb:KGW oscillator", Lith. J. Phys. 53(1), 41 –56 (2013).

[13] Melninkaitis, A., tolenis, T., Mažulė, L., Mirauskas, J., Sirutkaitis, V., Mangote, B., Fu, X., Zerrad, M., Gallais, L., Commandré, M., Kičas, S. and Drazdys, R., "Characterization of zirconia- and niobia-silica mixture coatings produced by ion-beam sputterin", Appl. Opt. 50(9), C188-C196 (2011).